

A Comparative Study of Fractional Quantum Hall Effect in Monolayer and Bilayer Graphene

¹S. Sahoo, ²A. K. Dutta

^{1,2} Department of Physics, National Institute of Technology, Durgapur – 713209, West Bengal, India.

¹ sukadev.sahoo4@gmail.com

² atanu.30255@gmail.com

ABSTRACT

Monolayer and bilayer of graphene are new classes of two-dimensional electron systems with unconventional band structures. The relativistic nature of electrons in graphene modifies the interelectron interactions. The fractional quantum Hall effect (FQHE), a distinct signature of interacting electrons in the system, can be realized as a manifestation of the integer quantum Hall effect (IQHE) of composite fermions consists of electrons bound to an even number of flux quanta. In this paper, we comparatively study the FQHE in monolayer and bilayer graphene.

Keywords: Graphene, Landau level, Composite fermion, Fractional quantum Hall effect.

1. INTRODUCTION

Monolayer grapheme (MLG) [1] is a monatomic sheet of carbon atoms. In this two-dimensional nonmaterial the carbon atoms are arranged in a hexagonal lattice and are covalently bonded by sp^2 hybridization. The honey comb lattice of monolayer grapheme consists of two interpenetrating triangular sub lattices. Whereas bilayer grapheme (BLG) [2] consists of two weakly van der Waals coupled honeycomb sheets of covalent-bond carbon atoms in a Bernal AB stacking. The system can be described in terms of four sub lattices, labeled A, B (upper layer) and C, D (lower layer). The A and C sites are coupled via a nearest-neighbor interlayer hopping term t . This hopping term describes the strength of inter-layer coupling. For $t = 0$ the two layers of grapheme are decoupled and bilayer system becomes identical to monolayer with additional double degeneracy. Electrons in monolayer grapheme behave as mass less two-dimensional fermions whereas electrons in bilayer grapheme behave as massive two-dimensional fermions [1,3]. The density of states D as a function of particle number (or particle density) n is found to be $D(n) \sim n^{1/2}$ for mass less two-dimensional fermions (electrons in monolayer grapheme) and $D(n) \sim \text{constant}$ for massive two-dimensional fermions (electrons in bilayer grapheme).

Formulae for density of states are $D = \frac{1}{\hbar v_F} \sqrt{\frac{g n}{\pi}}$

(mass less) and $D = \frac{g m^*}{2 \pi \hbar^2}$ (massive), where $g =$

degeneracy, and m^* is the effective mass of electrons. Thus, density of states depends upon particle density in monolayer grapheme but it is independent of particle density in bilayer grapheme. Mass less particles (e.g. photons) have energies which depend linearly on quantum number, while the energies of massive particles (e.g. free electrons) depend quadratic ally on quantum number. The mass less and massive dispersion relations in monolayer grapheme and bilayer grapheme respectively are: $E = \hbar v_F |\vec{k}|$ (mass less) and

$E = \frac{\hbar^2 k^2}{2 m^*}$ (massive), where $\hbar = h/2\pi$, h is the

Planck's constant, \vec{k} is the wave vector and v_F is the Fermi velocity of mass less electrons in the monolayer grapheme. Thus, each dispersion relation is characterized by a single parameter: v_F for mass less

dispersion, $v_F = (1.09 \pm 0.01) \times 10^6$ m/s and m^* for

the massive dispersion, $m^* = (0.0315 \pm 0.0001)m_e$,

m_e is the mass of electron. The hilarity of carriers in grapheme is associated with the Berry phase π in monolayer but 2π in bilayer grapheme. Moreover, the mass less character of the charge carriers in monolayer grapheme gives a \sqrt{B} dependence to the Landau levels (LL) whereas in bilayer grapheme the LL energy spectrum depends upon the magnetic field B linearly. The Landau levels are quantized energy levels for electrons in a magnetic field. Considering spin and valley degeneracy's, the zero-energy LL in a bilayer grapheme is 8-fold degenerate whereas it is 4-fold

<http://www.ejournalofscience.org>

degeneracy for other bilayer states. But it is 4-fold degeneracy for all LLs in a monolayer grapheme. The structure and degeneracy's of Landau level spectrum in a bilayer determine the sequences of QHE conductivity σ_{xy} which is different from that of monolayer grapheme and conventional semiconductor structures [4].

In recent experiments [5], the integer quantum Hall effect (IQHE) is observed in monolayer grapheme. It is found [5–8] that the Hall

$$\text{conductivity } \sigma_{xy} = \pm 4 \left(n + \frac{1}{2} \right) \frac{e^2}{h}, \text{ where } n \text{ is}$$

the Landau level index and the factor 4 accounts for grapheme's double spin and double band (valley) degeneracy. That is why; it is characterized as half-integer quantum Hall effect. The first plateau occurs at

$2e^2/h$. The half-integer QHE in monolayer grapheme

has also been suggested by theory groups [8,9]. This anomalous QHE is the direct evidence for Dirac fermions in monolayer grapheme. The IQHE in bilayer grapheme [4,10–12] is more interesting. Interestingly the first plateau at $n = 0$ is absent and the first plateau

appears at $4e^2/h$ like the conventional QHE,

characteristic of two-dimensional semiconductor systems [13–15]. In general, the quantized plateaus

appear at the standard sequence $\sigma_{xy} = \pm 4ne^2/h$

(same as the nonrelativistic electrons) with a missing plateau at zero energy [3], so that the step in the Hall conductance separating electron- and hole- like regions is twice as large as the quantized steps on either side of the charge neutral state. This anomaly at $E = 0$ can be removed by field effect doping, which has the effect of adding carriers and splitting the layer degeneracy of the zero energy Landau level producing two new steps in the

Hall conductance, each of height $4e^2/h$. This unusual quantization in bilayer grapheme leads new elementary excitations called massive Dirac fermions. These fermions have quadratic dispersion, like massive nonrelativistic particles, and described by an off diagonal, Dirac like Hamiltonian [3,16]. Thus we can say half-integer and full-integer QHE are shown in monolayer grapheme and bilayer grapheme respectively. The magnitude of Hall conductivity of the first plateau for bilayer grapheme is twice the corresponding value of monolayer grapheme.

A composite fermion [17] is an electron bound to an even number ($2m$) of flux quanta. These composite fermions make cyclotron motion in reduced effective magnetic field $B_{\perp}^{eff} = B_{\perp} - 2m\Phi_D\rho$, fill their own Landau levels, and generate an integer QH state at effective filling factor ν_{eff} (where ρ is the electronic

density in the lowest Landau level and $\Phi_D = 2\pi\hbar/e$ the Dirac flux quantum) [15]. It is the fractional QH state at filling factor $\nu = \nu_{eff} / (2m\nu_{eff} + 1)$. The filling

factor is defined as the ratio of total number of electrons to the total number of magnetic flux quanta (or the ratio between the electron density to the magnetic flux density). The FQHE in monolayer grapheme has been explored theoretically in a number of papers [18–25]. Recent experiments confirmed the existence of that effect in suspended monolayer grapheme samples [26,27] and in a single-layer grapheme sample fabricated on a hexagonal boron nitride (h-BN) substrate [28]. Recently theoretical studies of FQHE in bilayer grapheme [29–31] have been reported. The bilayer grapheme is a better candidate to observe FQHE than monolayer grapheme [29]. In this paper, we comparatively study the FQHE in monolayer and bilayer grapheme.

This paper is organized as follows: in Section 2, we obtain the analytical expressions for the Landau level energy spectrum of conventional two-dimensional electron system (2DES), monolayer and bilayer grapheme in magnetic field. In Section 3, we discuss FQHE in monolayer and bilayer grapheme. In section 4, we discuss our results and compared with others.

2. LANDAU LEVEL ENERGY SPECTRUM OF MONOLAYER AND BILAYER GRAPHENE IN MAGNETIC FIELD

In two dimensions, when electrons are subjected to a perpendicular magnetic field they follow close cyclotron orbits that in quantum mechanics are quantized. The energy of these orbitals has discrete values. These orbitals are called Landau Levels (LLs). The number of electrons per Landau level is directly proportional to the strength of the applied magnetic field. At strong magnetic field each LL is highly degenerate (i.e. there are so many states which have the same energy) and each LL has so many states that all of the free electrons in the system stay only in some LLs.

In case of conventional 2-dimensional electron system (non relativistic case) the Hamiltonian of a system is given by

$$H = \frac{p^2}{2m} \quad (1)$$

But in case of monolayer grapheme (relativistic case)

$$H = \vec{v} \begin{bmatrix} 0 & p_x - ip_y \\ p_x + ip_y & 0 \end{bmatrix} = \vec{v} \vec{p} \sigma, \quad (2)$$

where σ = Pauli matrix

$$\sigma^x = \begin{bmatrix} 0 & 1 \\ 1 & 0 \end{bmatrix}, \sigma^y = \begin{bmatrix} 0 & -i \\ i & 0 \end{bmatrix}, \text{ and} \\ \sigma^z = \begin{bmatrix} 1 & 0 \\ 0 & -1 \end{bmatrix} \quad (3)$$

http://www.ejournalofscience.org

and in bilayer graphene (relativistic case)

$$H = \frac{1}{2m} \begin{bmatrix} 0 & (p_x - ip_y)^2 \\ (p_x + ip_y)^2 & 0 \end{bmatrix}. \quad (4)$$

Let us apply the magnetic field to a monolayer (bilayer) graphene sheet taken in the xy plane, we assume that the magnetic field is homogeneous and given by

$$\vec{B} = \vec{\nabla} \times \vec{A}, \quad (5)$$

where, \vec{A} is the magnetic vector potential. The momentum is replaced by the gauge invariant form $\vec{\pi} = \vec{p} - e\vec{A}$ and $H(\vec{p}) \rightarrow H(\vec{\pi}) = H(\vec{p} - e\vec{A})$. Thus in presence of magnetic field the effective Hamiltonian for nonrelativistic case is given by,

$$H_{NR} = \frac{[\vec{p} - e\vec{A}]^2}{2m} \quad (6)$$

and for the monolayer grapheme

$$H_{MLG} = \frac{\vec{v}}{2m} \begin{bmatrix} 0 & \pi_x - i\pi_y \\ \pi_x + i\pi_y & 0 \end{bmatrix} \sigma \quad (7)$$

Similarly, in the presence of magnetic field the effective Hamiltonian for bilayer graphene is given by

$$H_{BLG} = \frac{1}{2m^*} \begin{bmatrix} 0 & (\pi_x - i\pi_y)^2 \\ (\pi_x + i\pi_y)^2 & 0 \end{bmatrix}, \quad (8)$$

where m^* is the effective mass of BLG. Equation (7) can be written as

$$H_{MLG} = \begin{bmatrix} 0 & A^\dagger \\ A & 0 \end{bmatrix},$$

where, $A^\dagger = \vec{v}(\pi_x - i\pi_y)$
 $A = \vec{v}(\pi_x + i\pi_y)$
 $= \vec{v} \sqrt{\frac{2eB}{\hbar}} \sqrt{\frac{\hbar}{2eB}} (\pi_x + i\pi_y)$
 $= \omega' \frac{\ell_B}{\sqrt{2}} (\pi_x + i\pi_y). \quad (9)$

Here, $\omega' = \vec{v} \sqrt{\frac{2eB}{\hbar}}$ and $\ell_B = \sqrt{\frac{\hbar}{eB}}$ is called magnetic length

$$A = \hbar \omega' \frac{\ell_B}{\sqrt{2}\hbar} (\pi_x + i\pi_y) \quad (10)$$

$$= \hbar \omega' a^\dagger$$

Similarly, we get $A^\dagger = \hbar \omega' a$

$$\text{Here, } a^\dagger = \frac{\ell_B}{\sqrt{2}\hbar} (\pi_x + i\pi_y) \quad (11)$$

$$\text{and } a = \frac{\ell_B}{\sqrt{2}\hbar} (\pi_x - i\pi_y) \quad (12)$$

are called ladder operators. And we have chosen appropriate normalization such that

$$[a, a^\dagger] = 1$$

Thus from the equation (11) and (12) we can write

$$\pi_x = \frac{\hbar}{\sqrt{2}\ell_B} (a^\dagger + a) \quad (13)$$

$$\pi_y = \frac{\hbar}{i\sqrt{2}\ell_B} (a^\dagger - a) \quad (14)$$

A. Conventional 2-dimensional electron system (Non-relativistic case)

For non-relativistic case the Hamiltonian in the presence of magnetic field becomes

$$H_{NR} = \frac{1}{2m} (\pi_x^2 + \pi_y^2)$$

Thus using the equations (13) and (14) we get

$$\begin{aligned} &= \frac{1}{2m} \left[\frac{\hbar^2}{2\ell_B^2} \left\{ (a^\dagger + a)^2 + \frac{1}{i^2} (a^\dagger - a)^2 \right\} \right] \\ &= \frac{1}{2m} \frac{\hbar^2}{2\ell_B^2} \left[(a^{\dagger 2} + a^2 + a^\dagger a + a a^\dagger) - (a^{\dagger 2} + a^2 - a^\dagger a - a a^\dagger) \right] \\ &= \frac{1}{4m} \frac{\hbar^2}{\ell_B^2} [2(a^\dagger a + a a^\dagger)] \\ &= \frac{\hbar^2}{2m\ell_B^2} [(a^\dagger a + a a^\dagger)] \\ &= \frac{\hbar^2}{2m\ell_B^2} [(a^\dagger a + a a^\dagger + a a^\dagger - a a^\dagger)] \\ &= \frac{\hbar^2}{2m\ell_B^2} [2a^\dagger a + 1] \quad [\text{using } [a, a^\dagger]=1] \\ &= \frac{\hbar^2}{m\ell_B^2} \left[a^\dagger a + \frac{1}{2} \right] \\ &= \frac{\hbar^2 eB}{m\hbar} \left[a^\dagger a + \frac{1}{2} \right] \quad [\text{putting the value of } \ell_B^2] \\ &= \frac{\hbar eB}{m} \left[a^\dagger a + \frac{1}{2} \right] \\ H_{NR} &= \frac{\hbar eB}{m} \left[a^\dagger a + \frac{1}{2} \right] \quad (15) \end{aligned}$$

Thus we get the energy eigenvalue as

$$E_n = \frac{\hbar eB}{m} \left[n + \frac{1}{2} \right] \quad (16)$$

<http://www.ejournalofscience.org>

This is the expression for LL energy spectrum for conventional 2D electron system. In this case, Landau quantization produces equidistant energy levels [11] which is due to the parabolic dispersion law of free electrons. The lowest state lies at finite energy $\hbar \omega_c / 2$, where cyclotron frequency $\omega_c = eB / m$.

B. Monolayer graphene

In the presence of magnetic field the effective Hamiltonian for monolayer graphene [19,29] is given by

$$H_{MLG} = \vec{v} \begin{bmatrix} 0 & (\pi_x - i\pi_y) \\ (\pi_x + i\pi_y) & 0 \end{bmatrix} \\ = \vec{v} \frac{\hbar\sqrt{2}}{\ell_B} \begin{bmatrix} 0 & a \\ a^\dagger & 0 \end{bmatrix} = \omega' \hbar \begin{bmatrix} 0 & a \\ a^\dagger & 0 \end{bmatrix} \quad (\text{putting}$$

$$\text{value of } \omega' = \frac{v\sqrt{2}}{\ell_B} \quad (17)$$

In perpendicular magnetic field the Hamiltonian generates a discrete Landau Level energy spectrum. The corresponding eigenfunctions can be expressed in terms of the conventional nonrelativistic Landau functions. The eigenvalue equation

$$H_{MLG} \Psi_n = E_n \Psi_n, \quad (18)$$

where the wave functions $\Psi_n = \begin{bmatrix} u_n \\ v_n \end{bmatrix}$.

Hence from equation (18)

$$\omega' \hbar \begin{bmatrix} 0 & a \\ a^\dagger & 0 \end{bmatrix} \begin{bmatrix} u_n \\ v_n \end{bmatrix} = E_n \begin{bmatrix} u_n \\ v_n \end{bmatrix}. \quad (19)$$

From the equation (19) we get

$$\hbar \omega' a v_n = E_n u_n \quad (20)$$

$$\hbar \omega' a^\dagger u_n = E_n v_n \quad (21)$$

Multiplying equation (21) with (20)

$$\hbar^2 \omega'^2 a^\dagger a u_n v_n = E_n^2 u_n v_n \quad (22)$$

Solving equation (22) we get, the energy eigenvalue as

$$E_n^2 = (\hbar^2 \omega'^2) n$$

$$E_n = \pm \frac{\hbar v \sqrt{2n}}{\ell_B}$$

$$E_n = \pm \frac{\hbar v \sqrt{2n}}{\sqrt{\frac{\hbar}{eB}}} \quad (\text{putting the value of } \ell_B)$$

$$E_n = \pm \sqrt{2n \hbar e B v^2} \quad (23)$$

This is the expression for LL energy spectrum in case of monolayer graphene. This expression shows that, in contrast to the case of conventional 2DES, the Landau levels in monolayer graphene are not equidistant and the largest energy separation is between the zero and the first Landau level. Here the positive values correspond to the Dirac electrons (conduction band) and the negative values correspond to the Dirac holes (valance band) in the monolayer graphene. There is a single state E_0 at zero energy.

C. Bilayer graphene

In the presence of magnetic field, the effective Hamiltonian for bilayer graphene [29] is written in equation (8). This can be written as

$$H_{BLG} = \frac{1}{2m^*} \frac{2\hbar^2}{\ell_B^2} \begin{bmatrix} 0 & a^2 \\ (a^\dagger)^2 & 0 \end{bmatrix} \\ = \frac{\hbar^2 eB}{m^* \hbar} \begin{bmatrix} 0 & a^2 \\ (a^\dagger)^2 & 0 \end{bmatrix} \\ = \hbar \omega_c \begin{bmatrix} 0 & a^2 \\ (a^\dagger)^2 & 0 \end{bmatrix}. \quad (24)$$

Here, $\omega_c = \frac{eB}{m^*}$ with m^* is the effective mass of BLG. The eigenvalue equation can be written as

$$H_{BLG} \Psi_n = E_n \Psi_n, \quad (25)$$

where the wave functions $\Psi_n = \begin{bmatrix} u_n \\ v_n \end{bmatrix}$ (26)

Using equations (24) and (26) in equation (25) we can write

$$\hbar \omega_c \begin{bmatrix} 0 & a^2 \\ (a^\dagger)^2 & 0 \end{bmatrix} \begin{bmatrix} u_n \\ v_n \end{bmatrix} = E_n \begin{bmatrix} u_n \\ v_n \end{bmatrix} \quad (27)$$

From the equation (27) we get

$$\hbar \omega_c (a)^2 v_n = E_n u_n \quad (28)$$

$$\hbar \omega_c (a^\dagger)^2 u_n = E_n v_n \quad (29)$$

Multiplying equation (29) with (28)

$$\hbar^2 \omega_c^2 (a^\dagger)^2 (a)^2 u_n v_n = E_n^2 u_n v_n \quad (30)$$

Solving equation (30) we get, the energy eigenvalue as

$$E_n = \pm \hbar \omega_c \sqrt{n(n-1)} \quad (31)$$

This is the expression for LL energy spectrum in case of bilayer graphene. Here the positive values correspond to the Dirac electrons (conduction band) and the negative values correspond to the Dirac holes

<http://www.ejournalofscience.org>

(valance band) in the bilayer graphene. This sequence is linear in field, similar to the standard case, but it contains an additional zero – energy level, which is independent of the field. In this case two lowest states $E_0 = E_1$ lie at zero energy. The above discussions indicate that the zero-energy level needs to be treated differently from the other Landau levels in graphene [32].

3. FRACTIONAL QUANTUM HALL EFFECT IN MONOLAYER AND BILAYER GRAPHENE

In high magnetic field each electron captures an even number ($2m$) of quantized vertices to become a composite fermion (CF). The dynamics of composite fermions are described by an effective magnetic field given by:

$$B^* = B - 2\pi (2m) \rho / e, \quad (32)$$

where ρ is the electronic density in the lowest Landau level.

The composite particles do not feel the external field B but the effective field B^* . Therefore, the FQHE of electrons can be considered as an IQHE of these composite particles [17]. The Hall plateaus at fractional filling factors appear as at integer filling factors except for the trivial modification that now each electron carries with it $2m$ flux quanta.

For an electronic density ρ , an effective filling factor f^* for the composite particles can be written as [9]:

$$f^* = \frac{2\pi\rho}{eB^*}. \quad (33)$$

In the lowest Landau level the electron filling factor is:

$$f = \frac{2\pi\rho}{eB}. \quad (34)$$

Using Eq. (33) in Eq. (32), we can write

$$B^* = B - 2mf^*B^*$$

$$\text{Or, } B = B^* (1 + 2mf^*). \quad (35)$$

From Eqs. (33), (34) and (35), we can write

$$\frac{f}{f^*} = \frac{B^*}{B} = \frac{1}{1 + 2mf^*} \quad (36)$$

$$\text{Or, } f = \frac{f^*}{1 + 2mf^*} \quad (37)$$

From the recent results [8,9,33] about the IQHE in monolayer graphene, the quantized Hall conductivity is found to be

$$\sigma_{xy} = \pm 2(2n+1) \frac{e^2}{h} \equiv \pm 4 \left(n + \frac{1}{2} \right) \frac{e^2}{h}, \quad (38)$$

where n is an integer. Here, the factor 2 is due to the spin degeneracy.

In the case of monolayer graphene the effective filling factor f^* is associated with the integer quantum Hall effect of composite particles and if we ignore the spin then we can write:

$$f^* = (2n + 1), \quad n = 0, 1, 2, 3, \dots \quad (39)$$

We disregard the spin of the electron, which brings additional two fold degeneracy of the Landau levels due to spin. Because we are working with electrons in magnetic field, this degeneracy is actually splitted by the Zeeman interaction [34].

Each filled single-degenerate Landau level contributes one conductance quantum e^2/h towards the observable Hall conductivity. Hence, the quantized Hall conductivity of monolayer graphene in FQHE [9,25] can be written as

$$\sigma_{xy} = \pm \frac{2n+1}{2m(2n+1)+1} \frac{2e^2}{h}. \quad (40)$$

Here the positive values correspond to the Dirac electrons (conduction band) and the negative values correspond to the Dirac holes (valance band) in the monolayer graphene.

Similarly, the quantized Hall conductivity of bilayer graphene in IQHE is found to be

$$\sigma_{xy} = \pm 4n \frac{e^2}{h} \equiv \pm 2 \times 2n \frac{e^2}{h}, \quad (41)$$

http://www.ejournalofscience.org

where n is an integer, $|n| \geq 1$ [10,16]. If we ignore spin like monolayer case we can write

$$f^* = 2n, n = 1, 2, 3, \dots \quad (42)$$

Hence, the quantized Hall conductivity of bilayer graphene in FQHE can be written as

$$\begin{aligned} \sigma_{xy} &= \pm \frac{2n}{1 + 2m \times 2n} \frac{2e^2}{h} \\ &= \pm \frac{4n}{1 + 4mn} \frac{e^2}{h}, \end{aligned} \quad (43)$$

where $m, n = 1, 2, 3, \dots$. Here the positive values correspond to the Dirac electrons (conduction band) and the negative values correspond to the Dirac holes (valance band) in the bilayer graphene.

4. RESULTS AND DISCUSSIONS

a. Monolayer graphene:

Now consider the equation (40) which represents the quantized Hall conductivity of monolayer graphene in FQHE.

(a) For $m = 0$, equation (40) becomes equation (38) which represents the quantized Hall conductivity in

IQHE in monolayer graphene. Thus we can say that the IQHE observed in monolayer graphene is a special case of its FQHE.

(b) For $n = 0$, equation (40) becomes

$$\sigma_{xy} = \pm \frac{1}{(2m + 1)} \frac{2e^2}{h}. \quad (44)$$

This equation explains the Laughlin sequence [35].

(c) Using equation (40) we calculate the quantized Hall conductivity of fractional quantum Hall effect in monolayer graphene. We have used the

standard value of $\frac{h}{e^2} = 25813 \Omega$ [36]. Hence $\frac{e^2}{h} =$

$3.874 \times 10^{-5} \Omega^{-1}$. We use $n \geq 0$ and $m > 0$. The corresponding values of filling factors are found to be $\pm 2/3, \pm 2/5, \pm 2/7, \pm 2/9, \pm 6/7, \pm 6/13, \pm 6/19, \pm 6/25, \pm 10/11, \pm 10/21, \pm 10/31, \pm 10/41, \pm 14/15, \pm 14/29, \pm 14/43, \pm 14/57, \pm 18/19, \pm 18/37, \pm 18/55, \pm 18/73, \dots$. Thus the FQHE in monolayer graphene has a sequence of states which is different from the sequence found in the conventional 2D electron gas. This is due to the special lattice structure of monolayer graphene and Dirac nature of carriers. Experimentally different filling factors are achieved by varying the applied magnetic field at a fixed electron concentration. The values of Hall conductivity are calculated in Table 1.

Table 1: Calculation of filling factors and quantized Hall conductivity of monolayer graphene

n	m	$\nu = \pm \frac{2(2n+1)}{1+2m(2n+1)}$	$\sigma_{xy} = \nu \frac{e^2}{h}$ (Ω^{-1})
0	1	$\frac{2}{3} = 0.667$	0.0000258
0	2	$\frac{2}{5} = 0.4$	0.0000155
0	3	$\frac{2}{7} = 0.286$	0.000011
0	4	$\frac{2}{9} = 0.222$	0.0000086
1	1	$\frac{6}{7} = .857$	0.0000332
1	2	$\frac{6}{13} = 0.462$	0.0000179
1	3	$\frac{6}{19} = 0.315$	0.0000122

<http://www.ejournalofscience.org>

1	4	$\frac{6}{25} = 0.24$	0.0000093
2	1	$\frac{10}{11} = 0.909$	0.0000351
2	2	$\frac{10}{21} = 0.476$	0.0000183
2	3	$\frac{10}{31} = 0.323$	0.0000125
2	4	$\frac{10}{41} = 0.244$	0.00000945
3	1	$\frac{14}{15} = 0.933$	0.0000362
3	2	$\frac{14}{29} = 0.482$	0.0000187
3	3	$\frac{14}{43} = 0.326$	0.0000126
3	4	$\frac{14}{57} = 0.246$	0.0000095
4	1	$\frac{18}{19} = 0.947$	0.0000367
4	2	$\frac{18}{37} = 0.486$	0.0000187
4	3	$\frac{18}{55} = 0.327$	0.0000127
4	4	$\frac{18}{73} = 0.247$	0.0000095

The variation of σ_{xy} with respect to different values of filling factors is shown in Fig. 1.

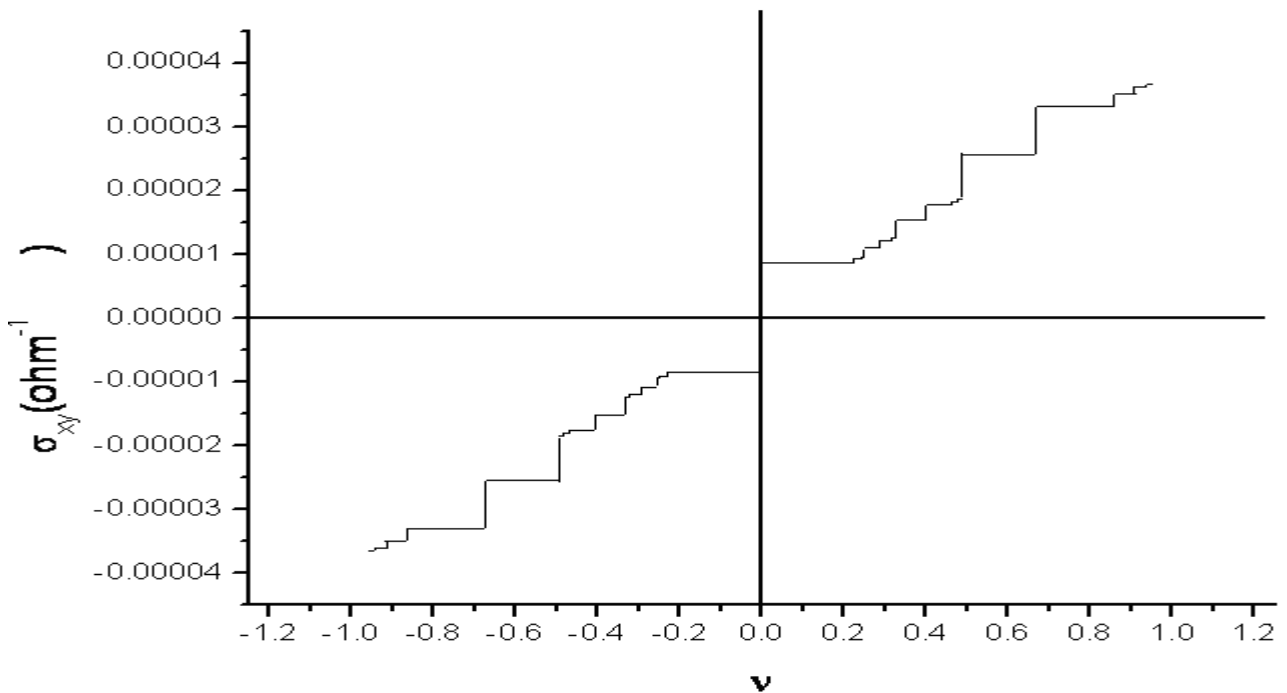


Fig. 1: Quantized Hall conductivity of monolayer graphene in fractional quantum Hall effect for different filling factors.

<http://www.ejournalofscience.org>

Apalkov and co-workers [21,37] investigated the energy spectra of the fractional quantum Hall states in monolayer graphene for a finite-size system. They have shown that the ground state of $\nu = 1/3$ and $1/5$ are spin and valley polarized at both $n = 0$ and $n = 1$ Landau levels. The fractional quantum Hall states were also studied in [29] within a numerical approach. They observed $\nu = 1/3, 2/3$, and $2/5$ fractional quantum Hall states. The FQHE has been recently observed experimentally [26, 27] in specially prepared suspended graphene samples. In such suspended samples, it was possible to observe FQHE at filling factor $1/3$. Very recently, the FQHE has been observed in a single-layer graphene sample fabricated on a hexagonal boron nitride (h-BN) substrate [28]. They have observed the FQHE at fractional filling factors $\nu = 1/3, 2/3$ and $4/3$ in the $n = 0$ Landau level and at $\nu = 7/3, 8/3, 10/3, 11/3$ and $13/3$ in the $n = 1$ Landau level.

b. Bilayer graphene:

Now consider the equation (43) which represents the quantized Hall conductivity of bilayer graphene in FQHE

(a) For $m = 0$, equation (43) becomes equation (41) which represents the quantized Hall conductivity of bilayer graphene in IQHE. Thus we can say that the IQHE observed in bilayer graphene is also a special case of its FQHE.

(b) Using equation (43), we calculate the quantized Hall conductivity of fractional quantum Hall effect in bilayer graphene. We use $n > 0$ and $m > 0$.

The corresponding values of filling factors (ν) are found to be $\pm 4/5, \pm 4/9, \pm 4/13, \pm 4/17, \pm 8/9, \pm 8/17, \pm 8/25, \pm 8/33, \pm 12/13, \pm 12/25, \pm 12/37, \pm 12/49, \pm 16/17, \pm 16/33, \pm 16/49, \pm 16/65, \pm 20/21, \pm 20/41, \pm 20/61, \pm 20/81, \dots$. In fact, in the present frame work QHE at fractional values of ν with odd denominators is as natural as the QHE at integer values of ν . One also expects weaker correlations for higher values of numerator. From our result it is clear that the FQHE in bilayer graphene has a sequence of states which is different from the sequence found in the conventional 2D electron gas and monolayer graphene. This is due to the unique properties of its charge carriers that are chiral fermions with a finite mass and the coupling between two graphene layers. The values of Hall conductivity are calculated in Table 2.

Table 2: Calculation of filling factors and quantized Hall conductivity of bilayer graphene

n	m	$\nu = \pm \frac{4n}{1 + 4mn}$	$\sigma_{xy} = \nu \frac{e^2}{h}$ (Ω^{-1})
1	1	$\frac{4}{5} = 0.8$	0.000031
1	2	$\frac{4}{9} = 0.444$	0.0000172
1	3	$\frac{4}{13} = 0.308$	0.0000119
1	4	$\frac{4}{17} = 0.235$	0.0000091
2	1	$\frac{8}{9} = 0.889$	0.0000344
2	2	$\frac{8}{17} = 0.471$	0.0000182
2	3	$\frac{8}{25} = 0.32$	0.0000124
2	4	$\frac{8}{33} = 0.242$	0.0000094
3	1	$\frac{12}{13} = 0.923$	0.0000358
3	2	$\frac{12}{25} = 0.48$	0.0000186
3	3	$\frac{12}{37} = 0.324$	0.0000126
3	4	$\frac{12}{49} = 0.245$	0.0000095
4	1	$\frac{16}{17} = 0.941$	0.0000365
4	2	$\frac{16}{33} = 0.485$	0.0000188

<http://www.ejournalofscience.org>

4	3	$\frac{16}{49} = 0.327$	0.0000126
4	4	$\frac{16}{65} = 0.246$	0.0000095
5	1	$\frac{20}{21} = 0.952$	0.0000369
5	2	$\frac{20}{41} = 0.488$	0.0000189
5	3	$\frac{20}{61} = 0.328$	0.0000127
5	4	$\frac{20}{81} = 0.247$	0.0000096

The variation of σ_{xy} with respect to different values of filling factors is shown in Fig. 2.

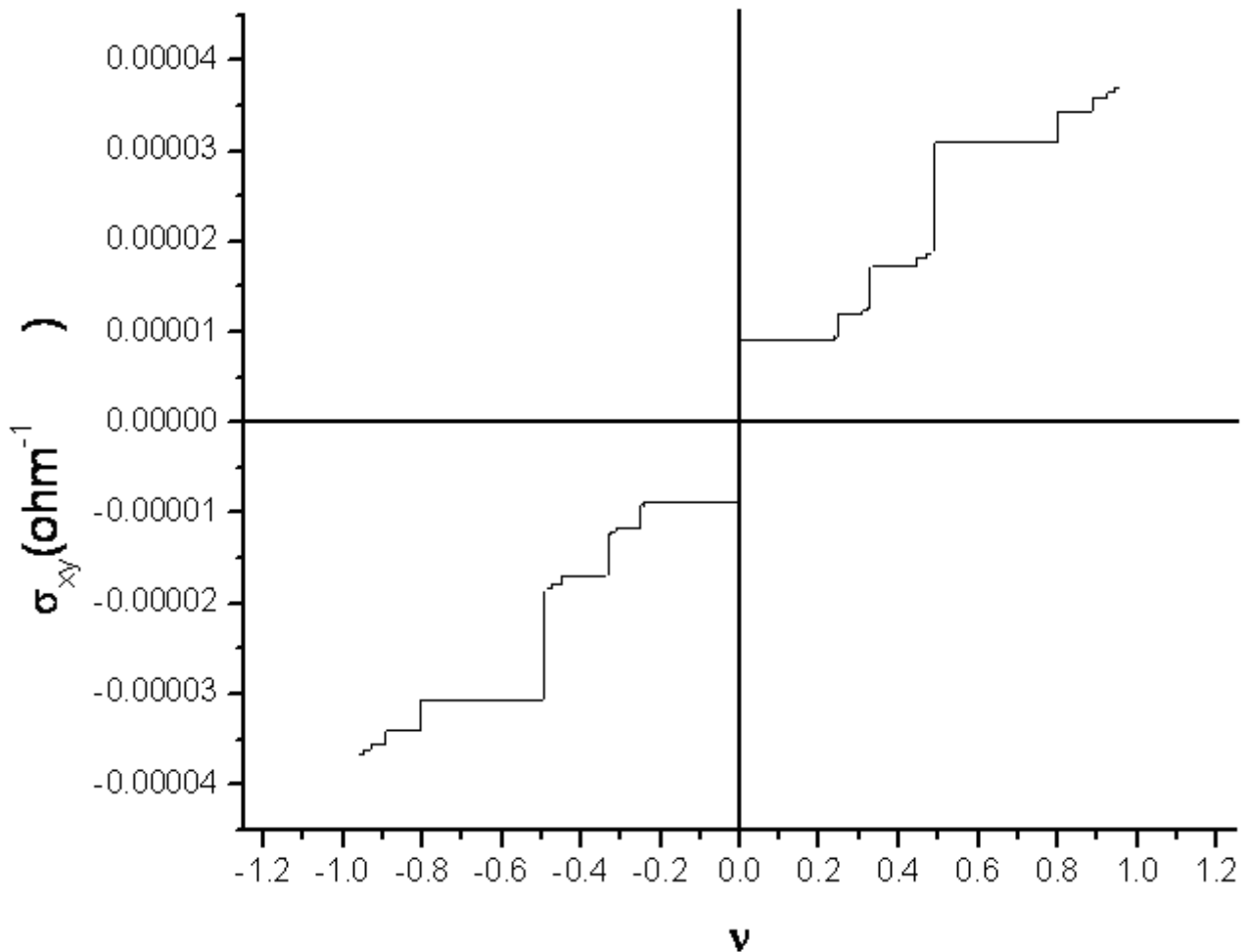


Fig. 2: Quantized Hall conductivity of bilayer graphene in fractional quantum Hall effect for different filling factors

A comparison of Hall conductivity between monolayer and bilayer graphene is shown in Fig. 3.

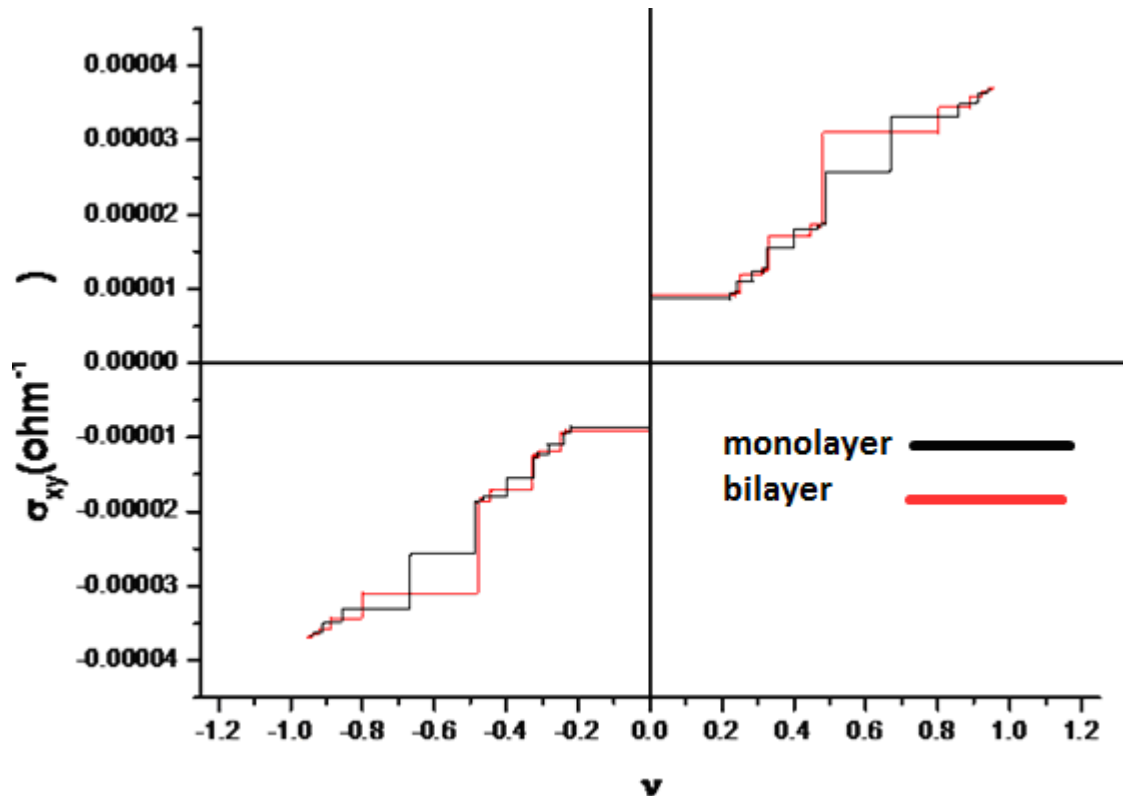


Fig. 3: A comparison of quantized Hall conductivity between monolayer and bilayer graphene in fractional quantum Hall effect for different filling factors.

The magnitude of Hall conductivity for bilayer graphene is more than the corresponding value of monolayer graphene.

Shibata and Nomura [29] investigated fractional Quantum Hall States on torus and spherical geometries by using the density matrix renormalization group (DMRG) method. They have found that at nonzero Landau level indices the ground states at $\nu = 1/3, 2/3$ and $2/5$ are valley polarized both in monolayer and bilayer graphene. In [30] the authors have studied FQHE in biased bilayer graphene. They observed fractional quantum Hall states at $\nu = 1/3$ and $2/5$. More interestingly, in our predicted filling factors $2/3$ and $2/5$ are present.

In conclusion, the FQHE in monolayer and bilayer graphene is among the most exciting observations in these new materials. The FQHE can be realized from the IQHE by adding an even number of flux quanta to each electron [17]. The FQHE observed in monolayer graphene is different from the conventional 2D electron gas. Similarly, the FQHE in bilayer graphene has a sequence of states which is different from the sequence found in the conventional 2D electron gas and monolayer graphene. Some of our predicted filling factors are matched with others predictions but most of

them are different. Our theoretical predictions may be checked theoretically and experimentally in future. The study of FQHE in monolayer and bilayer graphene is a very challenging field both theoretically and experimentally in condensed matter physics as well as quantum field theory.

REFERENCES

- [1] A. Hill, A. Sinner and K. Ziegler. 2010. arXiv: 1005.3211 [cond-mat.mtrl-sci].
- [2] M. Zarenia, J. M. Pereira Jr., F. M. Peters and G. A. Farias. 2009. arXiv: 0908.2831 [cond-mat.mes-hall].
- [3] S. Cho and M. S. Fuhrer. 2009. arXiv: 0901.41571 [cond-mat.mtrl-sci].
- [4] E. McCann and V. I. Fal'ko. 2006. Phys. Rev. Lett., 96, 086805. [arXiv: cond-mat/0510237 [cond-mat.mes-hall].
- [5] Y. Zhang, Y. W. Tan, H. L. Stormer, and P. Kim. 2005. Nature, 438, 201.
- [6] A. K. Geim and A. H. MacDonald. 2007. Physics Today, 60 (8), 35.

<http://www.ejournalofscience.org>

- [7] K. S. Novoselov, A. K. Geim, S. V. Morozov, D. Jiang, M. I. Katsnelson, I. V. Grigorieva, S. V. Dubonos, and A. A. Firsov. 2005. *Nature*, 438, 197.
- [8] V. P. Gusynin and S. G. Sharapov. 2005. *Phys. Rev. Lett.*, 95, 146801. [arXiv: cond-mat/0506575].
- [9] N. M. R. Peres, F. Guinea and A. H. Castro Neto. 2006. *Phys. Rev. B*, 73, 125411. [arXiv:cond-mat/0506709; arXiv: cond-mat/0512091].
- [10] K. S. Novoselov et al., 2006. *Nature Physics*, 2, 177.
- [11] D. S. L. Abergel, V. Apalkov, J. Berashevich, K. Ziegler and T. Chakraborty. 2010. *Advances in Physics*, 59(4), 261.
- [12] S. Das Sarma, S. Adam, E. H. Hwang and E. Rossi. 2010. ArXiv: 1003.4731 [cond-mat.mes-hall].
- [13] R. E. Prange and S. M. Girvin. 1990. *The Quantum Hall Effect*, Springer, New York.
- [14] A. H. Macdonald. 1990. *Quantum Hall Effect: A Perspective*, Kluwer Academic, Dordrecht.
- [15] Zyun F. Ezawa. 2008. *Quantum Hall Effects—Field Theoretical Approach and Related Topics*, World Scientific Publishing Co. Pte. Ltd., Singapore.
- [16] A. K. Geim and K. S. Novoselov,. 2007. *Nature Mater.* 6, 183.
- [17] J. K. Jain. 1989. *Phys. Rev. Lett.*, 63, 199; 1989. *Phys. Rev. B*, 40, 8074; 1990. *Phys. Rev. B*, 41, 7653.
- [18] J. Milton Pereira Jr., P. Vasilopoulos and F. M. Peeters. 2007. *Appl. Phys. Lett.* 90, 132122.
- [19] C. Töke, P. E. Lammert, V. H. Crespi and J. K. Jain. 2006. *Phys. Rev. B*, 74, 235417.
- [20] K. Yang, S. Das Sarma and A. H. MacDonald. 2006. *Phys. Rev. B*, 74, 075423 [arXiv: cond-mat/0605666].
- [21] V. M. Apalkov and T. Chakraborty. 2006. *Phys. Rev. Lett.*, 97, 126801.
- [22] C. Töke and J. K. Jain. 2007. arXiv: cond-mat/0701026.
- [23] M. O. Goerbig and N. Regnault. 2007. *Phys. Rev. B*, 75, 241405 [arXiv: cond-mat/ 0701661].
- [24] K. Yang,. 2007. *Solid State Commun.*, 143, 27 [arXiv:cond-mat/0703757].
- [25] S. Sahoo and S. Das. 2009. *Indian J. Pure & Appl. Phys.*, 47, 658.
- [26] X. Du, I. Skachko, F. Duerr, A. Luican and E. Y. Andrei. 2009. *Nature*, 462, 192.
- [27] K. I. Bolotin, F. Ghahari, M. D. Shulman, H. L. Stormer and P. Kim. 2009. *Nature*, 462, 196.
- [28] C. R. Dean *et al.*, 2010. arXiv: 1010.1179 [cond-mat.mes-hall].
- [29] N. Shibata and K. Nomura. 2009. *J. Phys. Soc. Japan*, 80, 104708; arXiv: 0906.1037 [cond-mat.str-el].
- [30] V. M. Apalkov and T. Chakraborty. 2010. *Phys. Rev. Lett.*, 105, 036801 [arXiv: 1007.4188 [cond-mat.mtrl-sci]].
- [31] V. M. Apalkov and T. Chakraborty. 2011. arXiv:1104.2020 [cond-mat.mes-hall].
- [32] M. O. Goerbig. 2011. arXiv:1104.5621 [cond-mat.mes-hall].
- [33] Z. Jiang, Y. Zhang, Y. W. Tan, H. L. Stormer and P. Kim. 2007. *Solid State Commun.*, 143, 14.
- [34] Z. Lenarčič. December 2010. Landau levels in graphene, a seminar talk at Ljubljana.
- [35] R. B. Laughlin. 1983. *Phys. Rev. Lett.*, 50, 1395.
- [36] M. O. Goerbig. 2009. ArXiv: 0909.1998 [cond-mat.mes-hall].
- [37] V. Apalkov, X.-F. Wang and T. Chakraborty. 2007. *Int. J. Mod. Phys. B.*, 21, 1165.